Reblur2Deblur: Deblurring Videos via Self-Supervised Learning

Huaijin Chen¹ Jinwei Gu² Orazio Gallo² Ming-Yu Liu² Ashok Veeraraghavan¹ Jan Kautz²

¹{huaijin.chen, vashok}@rice.edu ²{jinweig,ogallo,mingyul,jkautz}@nvidia.com

¹ Rice University ² NVIDIA



Figure 1. We propose a novel method for video motion deblur with self-supervised learning. Compared to prior method such as DVD [25] and DeblurGAN [13], we enforce a physics-based blur formation model during Deep Neural Network (DNN) learning, which effectively reduces image artifacts and improves generalization ability of DNN-based video deblurring.

Abstract

Motion blur is a fundamental problem in computer vision as it impacts image quality and hinders inference. Traditional deblurring algorithms leverage the physics of the image formation model and use hand-crafted priors: they usually produce results that better reflect the underlying scene, but present artifacts. Recent learning-based methods implicitly extract the distribution of natural images directly from the data and use it to synthesize plausible images. Their results are impressive, but they are not always faithful to the content of the latent image. We present an approach that bridges the two.

Our method fine-tunes existing deblurring neural networks in a self-supervised fashion by enforcing that the output, when blurred based on the optical flow between subsequent frames, matches the input blurry image. We show that our method significantly improves the performance of existing methods on several datasets both visually and in terms of image quality metrics.

1. Introduction

Cameras integrate scene radiance over a *finite* exposure time, which causes motion blur when the scene, the camera itself, or both move. Motion blur, in turn, affects the frequency content of the resulting image, thus hindering virtually any computer vision task. As a consequence, a number of deblurring algorithms have been proposed, which seek to estimate the latent, sharp image from one or more blurry

observations of a scene.

At high level, we can identify two classes of deblurring algorithms. *Physics-based methods* observe that blur can be modeled by a convolution of the latent image with a spatially varying filter, usually referred to as the blur kernel. Deblurring is then reduced to estimating the blur kernel and deconvolving it from the observed blurry image. Both the kernel estimation and the deconvolution process, however, are severely ill-posed and introduce artifacts, such as ringing artifacts [22].

A more recent trend is to use *deep-learning* methods to synthesize from blurry observations an image that best reflects the priors learned from training data [25, 13]. While neural networks have shown superior results in several fields of computer vision, they may require more training data than is available, and do become brittle when the training examples fail at capturing the full distribution of the real-world data. More importantly, while the synthesized images may be aesthetically pleasing, *e.g.*, sharper than the observations, they may not match the appearance of the latent image. Figure 1(c) shows one such example. The method by Kupyn *et al.* [13] reconstructs a sharp number "1," in place of the true number "3." This significantly reduces the benefit of using deep-learning based deblurring as a pre-processing step to computer vision algorithms.

Our method bridges the two approaches. Like previous methods, we use deep learning to synthesize sharp frames from a blurry video. However, we also explicitly enforce the solution to lie on the manifold of the sharp images that explain the observed blurry frames. To achieve this, we propose a self-supervised, end-to-end deblurring method. Our differentiable pipeline can be used to fine-tune any existing pre-trained network.

From multiple consecutive blurry video frames, we produce the corresponding sharp frames and estimate the optical flow between them. We use the flow information to compute a per-pixel blur kernel with which we reblur the sharp frames back onto the input images. By minimizing the distance between the synthesized blurry images and the input images, our approach allows to fine-tune the parameters of our network for specific inputs and without the need for the corresponding ground truth data. We show that our method outperforms the state-of-the-art methods based on both image quality metrics and visual inspection. Figure 1 shows two examples on which existing methods either fail or synthesize sharp estimates that do not reproduce the actual content of the latent sharp image. On the contrary, our method successfully recovers the ground truth image, while deblurring the input image.

2. Related Work

Traditionally, deblurring algorithms model the image formation as the convolution of a blur kernel with a sharp image, which is then estimated by means of deconvolution [15].

The blur kernel, however, is not straightforward to estimate. A common assumption is that the kernel is spaceinvariant [6, 22, 15], which is only valid when the scene is static—camera shake is the only source of motion blur—and planar. Even under this simplifying assumption, the problem is severely ill-posed, and thus requires regularization. Indeed several priors have been successfully employed for the latent image, e.g., TV [1], heavy-tailed gradient distribution [20], Gaussian distribution [14], smoothness [22], and for the shape of the kernel, e.g., sparsity of the kernel [6] or parametric kernel modeling [30]. Alternatively, the kernel can be estimated with a deep-learning approach [21, 2]. A few methods relax this assumption by estimating non-uniform blur kernels [28, 9, 27]. Several approaches move even further in this direction by leveraging optical flow or semantic segmentation to estimate a *per-pixel* blur [10, 7, 19].

The strength of these methods lies in their ability to explicitly model the physics of the image formation model. On the other hand, hand-crafted priors are not always realistic, and may result in visual artifacts in the estimated image.

An alternative way to tackle this problem is to learn directly from the data, which is possible thanks to the success of learning-based image synthesis approaches. Rather than estimating the blur kernel and explicitly deconvolving it from the observed image, these methods propose an end-to-end learning strategy to estimate the latent image.

To compensate for the lack of priors, some methods rely on video data [25, 29, 3]: because camera shake is an idiosyncratic motion, each frame can be thought as an independent observation of the scene.

In the absence of temporal information, a way to learn the priors is needed: Generative Adversarial Networks (GANs) are a powerful method for this task. Indeed a number of approaches successfully employ GANs to perform single-image deblurring [13, 18, 17].

Standard GAN-based methods have shown an extraordinary ability to learn the distribution of natural images. However, the images they synthesize, while realistic, may not reflect the input data accurately, as shown in Figure 1(c).

We propose to leverage the benefit of both approaches: after a kernel-free estimation of the latent image from multiple frames, we estimate the optical flow, and the per-pixel blur it induces. This allows us to *reblur* the estimated sharp images back on the observed blurry images, and to constrain the solution to the manifold of images that captures the *actual* input content.

3. Method

We propose to improve the performance of existing endto-end deblurring methods by encouraging solutions that more closely capture the content of the input image, in addition to being sharp. Our key idea is to introduce a physicsbased blur formation model into the DNN training, with which we *reblur* the estimated sharp images and minimize the difference with the input blurry images.

3.1. Overview and Notation

Given a deblur network $d(\cdot; \Theta_d)$, either pre-trained or trained from scratch, we estimate the latent sharp frame at time t, from the blurry observation $I_B^{(t)}$:

$$\hat{I}_{S}^{(t)} = d(I_{B}^{(t)}; \Theta_{d}).$$
 (1)

The weights of the deblurring network Θ_d can be learned by minimizing the loss $\mathcal{L}_{\mathcal{S}}$ over a dataset $\mathcal{S} = \{I_B; I_S\}$ with supervision

$$\mathcal{L}_{\mathcal{S}}(\Theta_d) = \sum_{\mathcal{S}} h(\hat{I}_S, I_S), \tag{2}$$

where $h(\cdot, \cdot)$ measures the distance between the estimated sharp images and the ground truth sharp images. The supervised loss $\mathcal{L}_{\mathcal{S}}(\Theta_d)$ can be computed with different choices of the distance function $h(\cdot, \cdot)$ [31], or with multiple input frames [25], or at multiple scales [16]. Recent work [18, 13, 16] introduced an additional GAN loss $\mathcal{L}_{\mathcal{G}}(\Theta_d)$, which achieved better performance by implicitly learning the distribution of sharp images. Relying solely on supervised learning, these methods still often produce image artifacts, especially when they are applied to images with different distributions of the training images.

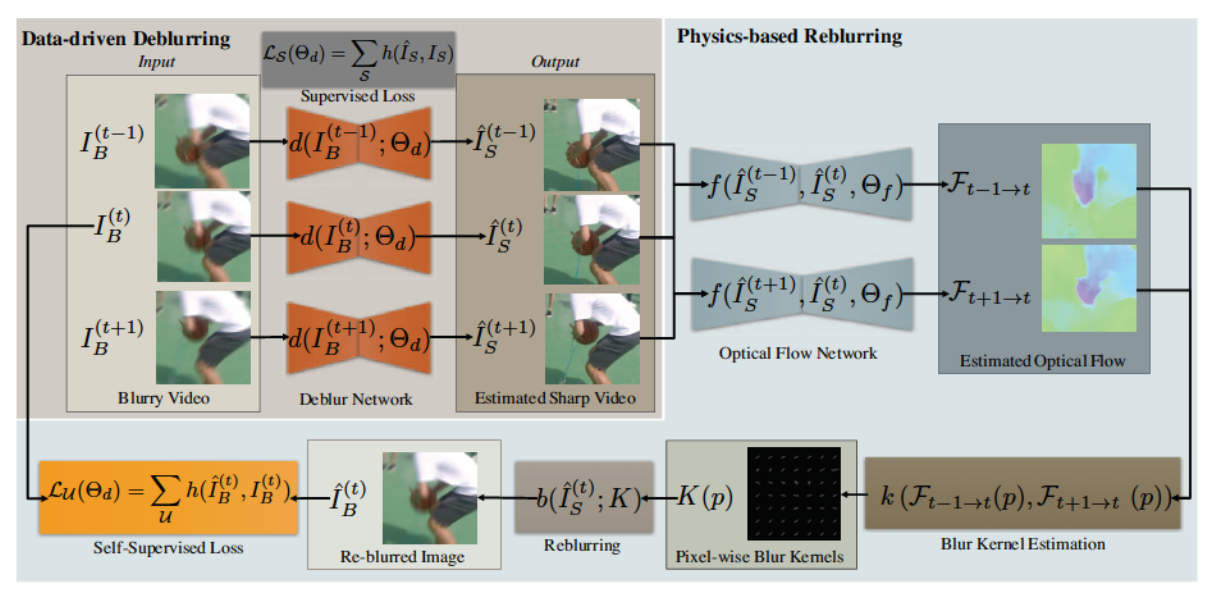


Figure 2. **System Overview**. Our proposed deblurring framework takes three consecutive blurry images as inputs. We first deblur each input image through the deblur network. After that, we compute the optical flow between the three recovered sharp images. We then estimate the per-pixel blur kernel and reconstruct the blurry input — this "reblurring" step offers an additional training signal for self-supervised learning to improve the deblur network and remove image artifacts.

Assume now that we are given a motion blurred video, rather than a single frame. By exploiting the motion information from videos, we incorporate a physics-based blur formation model into DNN learning to minimize image artifacts. Specifically, suppose we deblur three consecutive frames independently, obtaining $\{\hat{I}_S^{(t-1)}, \hat{I}_S^{(t)}, \hat{I}_S^{(t+1)}\}$. Since the frames are adjacent in time, we can compute the optical flow $\mathcal F$ between them. For this task we can use a different pre-trained neural network f:

$$\mathcal{F}_{t-1 \to t} = f(\hat{I}_S^{(t-1)}, \hat{I}_S^{(t)}, \Theta_f)$$
 (3)

$$\mathcal{F}_{t+1\to t} = f(\hat{I}_S^{(t+1)}, \hat{I}_S^{(t)}, \Theta_f).$$
 (4)

Recall that our method aims at removing *motion* blur: the optical flow $\mathcal{F}=(u,v)$, which expresses the motion at each pixel p, carries the necessary information to estimate a per-pixel blur kernel

$$K(p) = k \left(\mathcal{F}_{t-1 \to t} \left(p \right), \ \mathcal{F}_{t+1 \to t} \left(p \right) \right), \tag{5}$$

which serves an important function: it allows to close the loop with the original observation. If image $\hat{I}_S^{(t)}$ is estimated correctly, in fact, the corresponding reblurred image,

$$\hat{I}_{B}^{(t)} = b(\hat{I}_{S}^{(t)}; K), \tag{6}$$

should be close to the input blurry image $I_B^{(t)}$, where $b(\cdot;K)$ is the physics-based blur formation model.

This pipeline allows us to fine-tune the deblur network

 Θ_d over new blurry videos $\mathcal{U} = \{I_B^{(t)}\}$ by minimizing ¹

$$\mathcal{L}_{\mathcal{U}}(\Theta_d) = \sum_{\mathcal{U}} h(\hat{I}_B^{(t)}, I_B^{(t)}), \tag{7}$$

where $\mathcal{L}_{\mathcal{U}}(\Theta_d)$ is the self-supervised loss over the unlabeled videos \mathcal{U} . Equation (7) is precisely the mechanism by which we enforce that the estimated image $\hat{I}_S^{(t)}$ is consistent with the observed image $I_B^{(t)}$, in addition to following the distribution of natural, sharp images.

We implement all the three modules, *i.e.*, the debur network $d(\cdot; \Theta_d)$, the optical flow network $f(\cdot; \Theta_f)$, and the physics-based blur formation model $b(\cdot; K)$, to be differentiable, which allows an end-to-end training. Figure 2 shows the complete system pipeline. In the following sections we describe the implementation details of each module.

3.2. Deblur Network and Optical Flow Network

Our system can flexibly choose the deblur network $d(\cdot;\Theta_d)$ or the optical flow network $f(\cdot;\Theta_f)$. In this paper, for the deblur network, we evaluated two network architecture. The first one is DVD [25], which is an encoder-decoder architecture with skip connections. The second one is the generator part of DeblurGAN [13] which is also an encoder-decoder architecture, but with a global skip connection between the input layer and output layer to learn the image residuals, and nine "ResBlocks" [8] in the middle latent representation layers. For the optical flow network, we

 $^{^1\}mbox{We}$ can also simultaneously fine-tune the optical flow network Θ_f together with $\Theta_d.$

used FlowNetS [5] given its simplicity. Other variants can also be used, such as [26] and [11]. For the function $h(\cdot, \cdot)$ that measures the distance between two images, we used the MSE distance in the paper.

3.3. From Optical Flow to Reblurring

The physics-based blur formation model $b(\hat{I}_S; K)$ performs a per-pixel convolution with a spatially-varying blur kernel K(p) that is derived from the computed the optical flow $\mathcal{F}_{t-1 \to t}(p) = [u_{t-1 \to t}(p), v_{t-1 \to t}(p)]$ and $\mathcal{F}_{t+1 \to t}(p) = [u_{t+1 \to t}(p), v_{t-1 \to t}(p)]$, We assumed the same piecewise-linear motion blur kernel as proposed in [10] that consists of two line segments:

$$K(p)[x,y] = \begin{cases} \frac{\delta(-xv_{t+1 \rightarrow t}(p) + yu_{t+1 \rightarrow t}(p))}{2\tau||\mathcal{F}_{t+1 \rightarrow t}(p)||} & \text{if } (x,y) \in R_1\\ \frac{\delta(-xv_{t-1 \rightarrow t}(p) + yu_{t-1 \rightarrow t}(p))}{2\tau||\mathcal{F}_{t-1 \rightarrow t}(p)||} & \text{if } (x,y) \in R_2\\ 0 & \text{otherwise,} \end{cases}$$

where $R_1: x \in [0, \tau u_{t+1 \to t}(p)], y \in [0, \tau v_{t+1 \to t}(p)]$ and $R_2: x \in [0, \tau u_{t-1 \to t}(p)], y \in [0, \tau v_{t-1 \to t}(p)].$ τ is the exposure cycle as defined in [10], which is set to $\tau = 1$ in this paper.

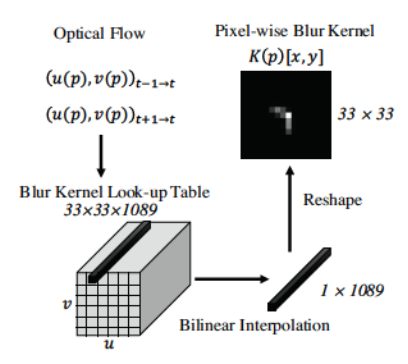


Figure 3. Optical Flow to Blur Kernel: We use a pre-computed lookup table and bilinear interpolation to convert the optical flow (u(p), v(p)) to per-pixel blur kernel K(p)[x, y]. This operation is differentiable, therefore can be instantiated as DNN layers.

The per-pixel blur kernel model defined above in Equation (8) cannot be directly used in DNN training, because the delta function $\delta(\cdot)$ is non-differentiable. To solve this issue, we use a precomputed lookup table that maps a set of optical flow values (u_i, v_i) to the blur kernels $k_i[x, y]$, where $i = 1, \dots, N$. For a given optical flow (u, v) at pixel p, we use bilinear interpolation to compute the blur kernel K(p)[x, y] from the lookup table:

$$K(p)[x,y] = \sum_{i=1}^{N} \omega_i(u,v)k_i[x,y].$$
 (9)

Table 1. Datasets used in our self-supervised fine-tuning experiments

Name	# Images Used	Description
MCD [16]	1111	GoPro, natural scenes
DVD [25]	150	GoPro/etc. cameras, natural scenes
ISOCHART	129	GoPro, ISO-Resolution chart
WFA [4, 3]	150	Blurry images only, natural scenes

Since the bilinear interpolation is differentiable with respect to the weights $\omega_i(u,v)$, the gradient can be back-propagated to the optical flow network $f(\cdot;\Theta_f)$ and, subsequently, to the deblur network $d(\cdot;\Theta_d)$. In this paper, we set $N=33\times 33$ to compute the lookup table, thus limiting the range of the optical flow to compute the motion blur kernels from -16 pixels to 16 pixels in both directions. Figure 3 shows a diagram of this procedure.

3.4. Other Implementation Details

For the fine-tuning step, we found that minimizing the self-supervised loss $\mathcal{L}_{\mathcal{U}}$ alone leads to degenerate solutions. Therefore, we use the hybrid loss

$$\mathcal{L}(\Theta_d) = \mathcal{L}_{\mathcal{S}}(\Theta_d) + \alpha \mathcal{L}_{\mathcal{U}}(\Theta_d), \tag{10}$$

which also includes the supervision loss $\mathcal{L}_{\mathcal{S}}$ from the original supervised datasets \mathcal{S} . Each mini-batch is sampled partially from the original supervised datasets \mathcal{S} and partially from the new unlabeled videos \mathcal{U} . The weight coefficient α balances the contribution of the self-supervision loss and the supervised loss. We set $\alpha=0.1$ in all our experiments.

We implemented our algorithm in PyTorch. For both the deblur network $d(\cdot;\Theta_d)$ and the optical flow network $f(\cdot;\Theta_f)$, we started from pre-trained models, which we refer to as baseline networks. We performed 200 self-supervised learning iterations on the baseline networks. We used the ADAM solver [12] with a learning rate of 0.0001 for all our experiments, and a learning rate decay of 0.5 applied at 30, 50, and 100 epochs. We set the training mini-batch size between 8 and 20 depending on the DNN memory footprint. Finally, we use NVIDIA TitanX GPUs for training and testing.

4. Experiments and Results

In this section, we describe the experiments we performed, including the datasets, network visualization, the quantitative and qualitative results, as well as a thorough ablation study. More results, including full-size images are available in the Supplementary.

4.1. Datasets and Baselines

We evaluated the proposed method extensively on four datasets, as summarized in Table 1. Both the MCD [16] and

DVD [25] datasets were captured with high-speed camera such as GoPro Hero 5 and Sony RX10 at 240fps, and thus have ground truth sharp images for quantitative evaluation. In addition, in order to test the generalization ability of deblurring algorithms (other than natural scenes), we also used a GoPro camera and captured a small dataset of an ISO-resolution chart moving in front of the camera. We refer to this as the ISOCHART set, which we will release upon publication. For these three datasets, we average every 9 frames to create the blurry image and use the center frame as the sharp ground truth. Finally, the WFA dataset [4, 3] is widely used for evaluating deblurring algorithms. It does not offer ground truth images and thus can only be evaluated qualitatively. Note that all these four datasets are used as the unsupervised dataset \mathcal{U} in our experiment, which means we use only the blurry images as the input for self-supervised learning.

As mentioned earlier, we compared with two recent methods as our baseline, the DVD [25], which is an autoencoder with skip connection for deblurring, and the Deblur-GAN [13], which is the generator part of a GAN network. These two methods are representative since one is purely supervised learning from blur-sharp pairs and the other incorporates the GAN loss. We applied the proposed self-supervised learning method on top of these two baselines and fine-tuned the networks. We refer to the resulting networks as DVD-Reblur and DeblurGAN-Reblur respectively. In addition, we also compared with the MCD [16] method, which is similar to DeblurGAN.

4.2. A Closer Look At Reblur2Deblur

Let us first take a closer look at the proposed network and visualize some intermediate outputs, in order to understand why and how it works. Figure 4 shows the optical flow and the deblurred images before and after the reblur finetuning. The blur in this example is caused only by camera motion, and thus the true optical flow should be smooth – the fine-tuning removes the artifacts due to the scene's texture from the original optical flow. Thus, by fine-tuning with the physics-based blur formation model, we improve both the deblur network Θ_d and the optical flow network Θ_f .

Figure 5 visualizes the saliency of the deblur network using guided back-propagation (GBP) [23, 24] before and after the reblur fine-tuning, where the red pixels have positive gradients and the green pixels have negative gradients. As shown, while both the baseline network and the fine-tuned network are able to capture important edge and corner pixels, the baseline network also pays attention to high-color-contrast pixels (*e.g.*, windows around the building) and thus introduces artifacts in the deblurred image. In contrast, the proposed reblur-based fine-tuning helps to focus more on the pixels around global edge/line/corner structures and remove such artifacts in the deblurred image.



Figure 4. Optical Flow in Reblur2Deblur. By fine-tuning via the physics-based blur formation model, we improve both the deblur network Θ_d and the optical flow network Θ_f . The blur in this example image is caused only by camera motion — the fine-tuning removes the artifacts in the optical flow (due to scene texture). The deblurred image of DeblurGAN-Reblur is also better than the baseline DeblurGAN.

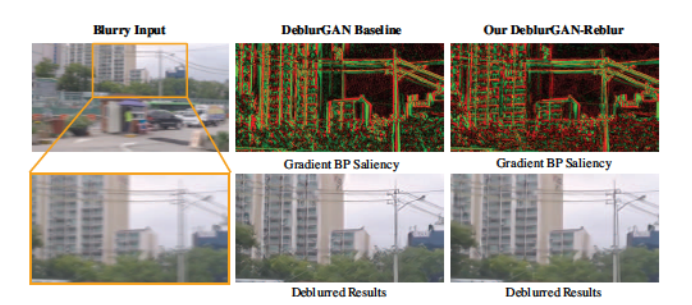


Figure 5. Saliency with Guided Back-propagation (GBP). We show the GBP saliency [24, 23] of the deblur network before and after the reblur fine-tuning, where red pixels have positive gradients and green pixels have negative gradients. The baseline network focuses more on high-color-contrast regions (e.g., windows in the building) and thus introduces artifacts in the deblurred image. The reblur-based fine-tuning guides the network to focus more on global edge/line/corner structures and removes such artifacts in the deblurred image.

4.3. Deblurring Results

Figure 6 shows several examples from the four datasets. Table 2 shows the averaged PSNR and SSIM for the three datasets. As shown, our proposed self-supervised learning method brings significant improvement over the two baseline networks (especially over the DeblurGAN-baseline, about 1 dB improvement). Both proposed methods DeblurGAN-Reblur and DVD-Reblur effectively remove the artifacts introduced by the networks by enforcing the physics-based blur formation model.

We also compared with the MCD network [16], which is a multi-scale network with a GAN loss. The average PSNR of MCD on the three datasets are 28.53, 31.21, and 32.30 respectively, which are slightly better than ours (DeblurGAN-Reblur). However as shown in Figure 6 and the supplementary material, we found DeblurGAN-Reblur often achieves

better visual quality than MCD (see the ISOCHART in Figure 6 for example). In addition, our proposed methods are computationally more efficient than MCD: MCD takes 4.33 seconds to deblur an image at resolution 1280×720 , while DeblurGAN-Reblur takes 0.85 second and DVD-Reblur takes 0.84 second to deblur at the same image resolution — about $5 \times$ faster run time than MCD.

4.4. Ablation Study

We also performed an ablation study to analyze several aspects of the proposed method. For computational efficiency, we ran all the studies over a randomly picked subset of the MCD dataset comprising 50 images.

Choices of the Blur Formation Model $b(\hat{I}_S^{(t)}; K)$ In addition to the blur formation model described in Section 3.3, which is based on per-pixel convolution, one can warp the estimated sharp image $\hat{I}_S^{(t)}$ towards t+1 and t-1 directly using the the optical flow $\mathcal{F}_{t+1 \to t}$ and $\mathcal{F}_{t-1 \to t}$, and average the resulting images. The warping can be implemented with bilinear interpolation, making this formation model also differentiable.

Table 5 summarizes the results. As shown, the per-pixel convolution blur formation model performs slightly better in terms of PSNR and SSIM, while the warping-based blur formation runs much faster during the fine-tuning. Nevertheless, both blur formation models produce significant improvement over the two baseline methods.

Self-supervised Learning on a Single Image Since the proposed method is self-supervised, in theory one can fine-tune the deblur network for each individual image separately, despite the high computational cost. Interestingly, we found this customized, single-image based fine-tuning to be not necessarily better — slightly worse, in fact — than fine-tuning over a group of testing images. Table 4 summarizes the results for five randomly picked images, each of which is fine-tuned separately with DeblurGAN-Reblur. One possible explanation is that fine-tuning over a set of testing images may produce a more stable gradient based on the underlying image distribution, and may thus be less likely to get stuck in local minima. The full-resolution results of these five images are provided in the Supplementary.

Effect of the number of frames in the blur formation model When we construct the physics-based blur formation model, we need to compute two optical flow maps $\mathcal{F}_{t+1\to t}$ and $\mathcal{F}_{t-1\to t}$, which requires at least three frames as input. In addition, we also experimented with only two frames as input, and made the assumption that $\mathcal{F}_{t+1\to t} \approx -\mathcal{F}_{t-1\to t}$. We evaluated with DVD-Reblur network. As

expected, we found that the three-frame based method performs better than the two-frame based method. Table 5 summarizes the results.

5. Conclusion and Discussion

In this paper, we proposed a novel deep learning based method for video motion deblurring. In order to improve the generalization ability and overcome the image artifacts of prior supervised-learning based methods, we propose to incorporate a physics-based blur formation model to reblur the estimated sharp images, which allows us to fine-tune the deblur network via self-supervised learning. We evaluated our method over multiple datasets and found the proposed approach effectively removes image artifacts and improves performance.

There are several limitations in the current approach that we plan to address in the future. While the piece-wise linear blur kernel based on optical flow is applicable for most motion blur in videos, this assumption does not hold for large amount of motion blur which often results in nonlinear, complex blur kernels. Moreover, the GAN-based training has been shown to learn the statistical distribution of images well — it can be also incorporated with the physics-based blur formation model for the self-supervised learning.

Acknowledgments

This work was done when Huaijin Chen was a summer intern in NVIDIA Research. Ashok Veeraraghavan and Huaijin Chen were also partially supported by NSF CAREER Award 1652633.

References

- José M Bioucas-Dias, Mario AT Figueiredo, and João Pedro Oliveira. Total variation-based image deconvolution: a majorization-minimization approach. In *IEEE International Conference on Acoustics, Speech and Signal Processing (ICASSP)*, 2006.
- [2] Ayan Chakrabarti. A neural approach to blind motion deblurring. In European Conference on Computer Vision (ECCV), pages 221–235, 2016. 2
- [3] Sunghyun Cho, Jue Wang, and Seungyong Lee. Video deblurring for hand-held cameras using patch-based synthesis. ACM Transactions on Graphics (TOG), 31(4):64, 2012. 2, 4, 5,7
- [4] Mauricio Delbracio and Guillermo Sapiro. Hand-Held video deblurring via efficient Fourier aggregation. *IEEE Transac*tions on Computational Imaging, 1(4):270–283, 2015. 4, 5, 7
- [5] Alexey Dosovitskiy, Philipp Fischer, Eddy Ilg, Philip Hausser, Caner Hazirbas, Vladimir Golkov, Patrick van der Smagt, Daniel Cremers, and Thomas Brox. FlowNet: Learning optical flow with convolutional networks. In *IEEE International* Conference on Computer Vision (ICCV), 2015. 4

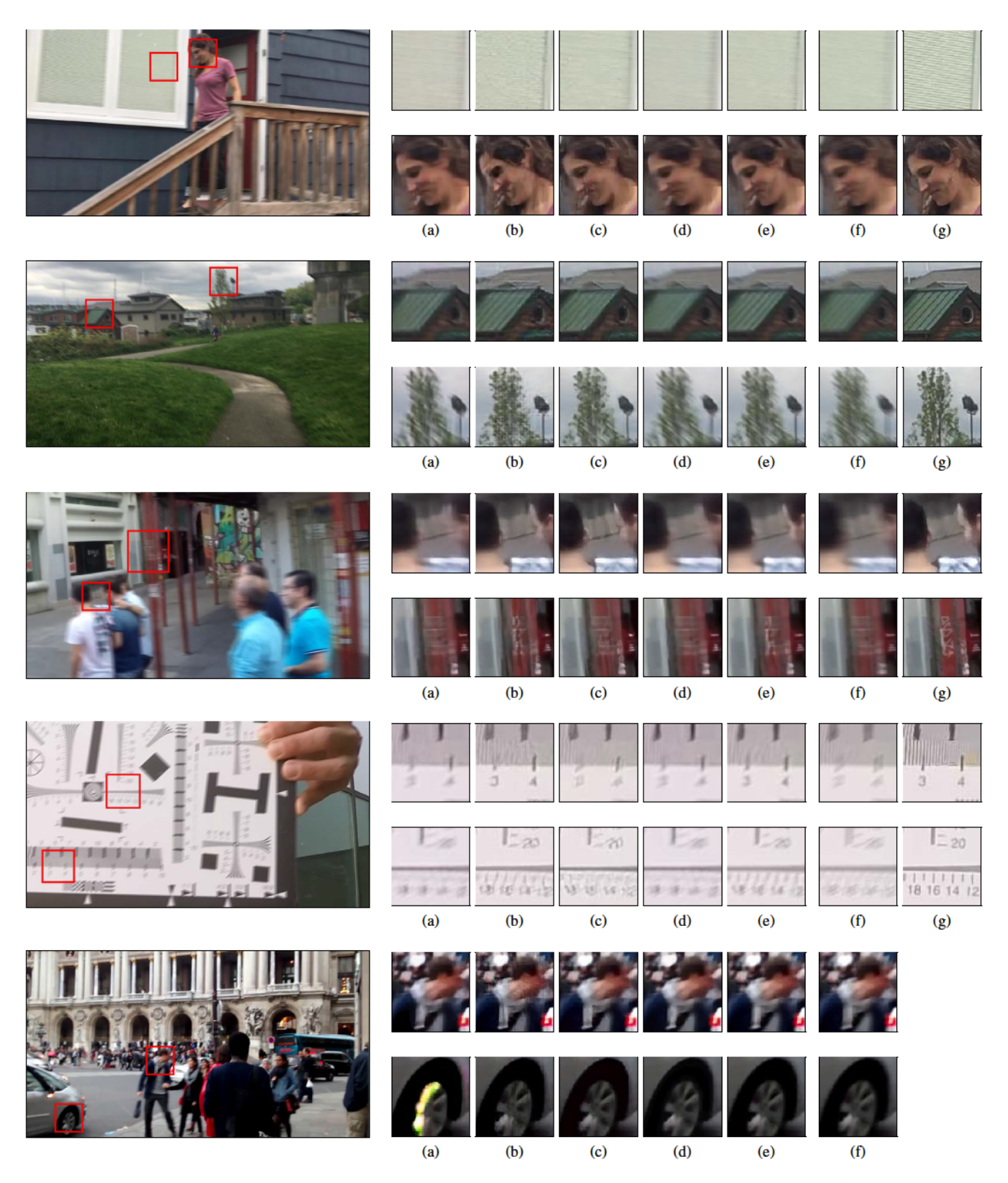


Figure 6. Comparison of several deblur methods on images from different datasets. The images are from DVD [25], MCD [16], WFA [4, 3] and our own ISOCHART datasets. The insets on the right shows the detailed input and deblur results of the bounding box areas in the left input images. The deblur results follow the order of (a) DVD baseline [25] (b) DeblurGAN [13], (c) MCD [16], (d) DVD-Reblur (ours), (e) DeblurGAN-Reblur (ours), (f) blurry (input), (g) ground truth. (The ground truth is not available for the WFA dataset, therefore the last column of the last row missing.) The complete, full resolution images are available in the supplementary material.

Table 2. Comparison of several state-of-art deblurring techniques (in terms of average PSNR, SSIM and average run-time) on three datasets. DVD-Reblur and DeblurGAN-Reblur are proposed methods which integrate the reblurring framework within existing DNN-based deblurring algorithms.

Network→ Datasets↓) [25] SSIM		Reblur SSIM	I	GAN [13]	Deblur(PSNR	GAN-Reblur
Datasets	I SINK	SOUVI	I SINK	SOUVI	LOINK	SOUVI	I SINK	SSIM
MCD	25.36	0.8380	26.06	0.8515	27.30	0.8954	28.32	0.9337
DVD	29.15	0.9218	30.15	0.9265	30.16	0.9364	31.37	0.9400
ISOCHART	29.85	0.9632	30.32	0.9706	31.89	0.9796	31.96	0.9814

Table 3. Results of two different blur formation models. The column "Time" is the average running time for fine-tuning a mini-batch of 10 RGB images of size 128×128 .

Network	PSNR	SSIM	Time (s)
DVD [25]	25.067	0.872	-
DVD-Reblur, Conv-Based	25.694	0.880	2.15
DVD-Reblur, Warp-Based	25.693	0.880	0.56
DeblurGAN [13]	26.884	0.913	-
DeblurGAN-Reblur, Conv-Based	27.531	0.923	2.32
DeblurGAN-Reblur, Warp-Based	27.529	0.922	1.01

Table 4. Fine-tuning deblur network on single image vs. on group of images. Each approach's resulting PSNR and SSIM are shown.

	Individual		Group		
Image No.	PSNR	SSIM	PSNR	SSIM	
1	26.538	0.878	27.004	0.894	
2	27.813	0.915	28.201	0.923	
3	23.783	0.843	23.776	0.844	
4	25.453	0.863	25.855	0.880	
5	24.316	0.886	25.231	0.910	

Table 5. Deblurring performance of three-frame based vs. two-frame based blur formation model.

Network	PSNR	SSIM
DVD [25]	25.067	0.872
DVD-Reblur (2 frames)	25.163	0.869
DVD-Reblur (3 frames)	25.694	0.880

- [6] Rob Fergus, Barun Singh, Aaron Hertzmann, Sam T Roweis, and William T Freeman. Removing camera shake from a single photograph. In ACM Transactions on Graphics (TOG), volume 25, pages 787–794, 2006.
- [7] Dong Gong, Jie Yang, Lingqiao Liu, Yanning Zhang, Ian Reid, Chunhua Shen, Anton van den Hengel, and Qinfeng Shi. From motion blur to motion flow: a deep learning solution for removing heterogeneous motion blur. arXiv preprint arXiv:1612.02583, 2016. 2
- [8] Kaiming He, Xiangyu Zhang, Shaoqing Ren, and Jian Sun. Deep residual learning for image recognition. In *IEEE conference on Computer Vision and Pattern Recognition (CVPR)*, 2016. 3
- [9] Michael Hirsch, Christian J Schuler, Stefan Harmeling, and

- Bernhard Schölkopf. Fast removal of non-uniform camera shake. In *IEEE International Conference on Computer Vision (ICCV)*, pages 463–470, 2011. 2
- [10] Tae Hyun Kim and Kyoung Mu Lee. Generalized video deblurring for dynamic scenes. In *IEEE Conference on Com*puter Vision and Pattern Recognition (CVPR), 2015. 2, 4
- [11] Eddy Ilg, Nikolaus Mayer, Tonmoy Saikia, Margret Keuper, Alexey Dosovitskiy, and Thomas Brox. FlowNet 2.0: Evolution of optical flow estimation with deep networks. arXiv preprint arXiv:1612.01925, 2016. 4
- [12] Diederik Kingma and Jimmy Ba. Adam: A method for stochastic optimization. arXiv preprint arXiv:1412.6980, 2014. 4
- [13] Orest Kupyn, Volodymyr Budzan, Mykola Mykhailych, Dmytro Mishkin, and Jiri Matas. DeblurGAN: blind motion deblurring using conditional adversarial networks. arXiv preprint arXiv:1711.07064, 2017. 1, 2, 3, 5, 7, 8
- [14] Anat Levin, Rob Fergus, Frédo Durand, and William T Freeman. Image and depth from a conventional camera with a coded aperture. ACM Transactions on Graphics (TOG), 26(3):70, 2007.
- [15] Anat Levin, Yair Weiss, Fredo Durand, and William T Freeman. Understanding and evaluating blind deconvolution algorithms. In *IEEE Conference on Computer Vision and Pattern Recognition (CVPR)*, 2009.
- [16] Seungjun Nah, Tae Hyun Kim, and Kyoung Mu Lee. Deep multi-scale convolutional neural network for dynamic scene deblurring. In *IEEE Conference on Computer Vision and Pattern Recognition (CVPR)*, 2017. 2, 4, 5, 7
- [17] T. M. Nimisha, Akash Kumar Singh, and A. N. Rajagopalan. Blur-invariant deep learning for blind-deblurring. In IEEE International Conference on Computer Vision (ICCV), 2017.
- [18] Sainandan Ramakrishnan, Shubham Pachori, Aalok Gangopadhyay, and Shanmuganathan Raman. Deep generative filter for motion deblurring. arXiv preprint arXiv:1709.03481, 2017.
- [19] Wenqi Ren, Jinshan Pan, Xiaochun Cao, and Ming-Hsuan Yang. Video deblurring via semantic segmentation and pixelwise nonlinear kernel. In *IEEE International Conference on Computer Vision (ICCV)*, 2017.
- [20] Stefan Roth and Michael J Black. Fields of experts: A framework for learning image priors. In *IEEE Conference on Com*puter Vision and Pattern Recognition (CVPR), pages 860–867, 2005. 2

- [21] Christian J Schuler, Michael Hirsch, Stefan Harmeling, and Bernhard Schölkopf. Learning to deblur. *IEEE Transactions on Pattern Analysis and Machine Intelligence (TPAMI)*, 38(7):1439–1451, 2016. 2
- [22] Qi Shan, Jiaya Jia, and Aseem Agarwala. High-quality motion deblurring from a single image. In *ACM Transactions on Graphics (TOG)*, volume 27, page 73, 2008. 1, 2
- [23] Karen Simonyan, Andrea Vedaldi, and Andrew Zisserman. Deep inside convolutional networks: Visualising image classification models and saliency maps. arXiv preprint arXiv:1312.6034, 2013. 5
- [24] Jost Tobias Springenberg, Alexey Dosovitskiy, Thomas Brox, and Martin Riedmiller. Striving for simplicity: The all convolutional net. arXiv preprint arXiv:1412.6806, 2014. 5
- [25] Shuochen Su, Mauricio Delbracio, Jue Wang, Guillermo Sapiro, Wolfgang Heidrich, and Oliver Wang. Deep video deblurring. In *IEEE Conference on Computer Vision and Pattern Recognition (CVPR)*, 2017. 1, 2, 3, 4, 5, 7, 8
- [26] Deqing Sun, Xiaodong Yang, Ming-Yu Liu, and Jan Kautz. PWC-Net: CNNs for optical flow using pyramid, warping, and cost volume. arXiv preprint arXiv:1709.02371, 2017. 4
- [27] Jian Sun, Wenfei Cao, Zongben Xu, and Jean Ponce. Learning a convolutional neural network for non-uniform motion blur removal. In *IEEE Conference on Computer Vision and Pattern* Recognition (CVPR), 2015. 2
- [28] Oliver Whyte, Josef Sivic, Andrew Zisserman, and Jean Ponce. Non-uniform deblurring for shaken images. *International Journal of Computer Vision (IJCV)*, 98(2):168–186, 2012.
- [29] Patrick Wieschollek, Michael Hirsch, Bernhard Scholkopf, and Hendrik P. A. Lensch. Learning blind motion deblurring. In *IEEE International Conference on Computer Vision* (ICCV), 2017. 2
- [30] Ruomei Yan and Ling Shao. Blind image blur estimation via deep learning. *IEEE Transactions on Image Processing (TIP)*, 25(4):1910–1921, 2016. 2
- [31] Hang Zhao, Orazio Gallo, Iuri Frosio, and Jan Kautz. Loss functions for image restoration with neural networks. *IEEE Transactions on Computational Imaging*, 3(1):47–57, 2017.